APPENDIX A: Survey of Existing Filament Stretching Experiments in Polymer Solutions

Over the past decade a number of investigators have used filament stretching rheometry to probe the transient extensional rheology of many different polymer solutions. These experiments have spanned a wide range of concentrations and molecular weights. The experimental conditions for each test fluid can be summarized succinctly in a double-logarithmic plot of the molecular weight of the polymer chain against its mass concentration (or weight fraction) in solution. Such a representation was first promulgated by Graessley (1980), and we thus refer to this as a *Graessley Diagram*. In Figure A.1 we summarize the experimental conditions of all existing published filament stretching data for polymer solutions and melts. The numerical values of the concentration and molecular weight plus the relevant literature citation for each fluid are compiled in Table A.1

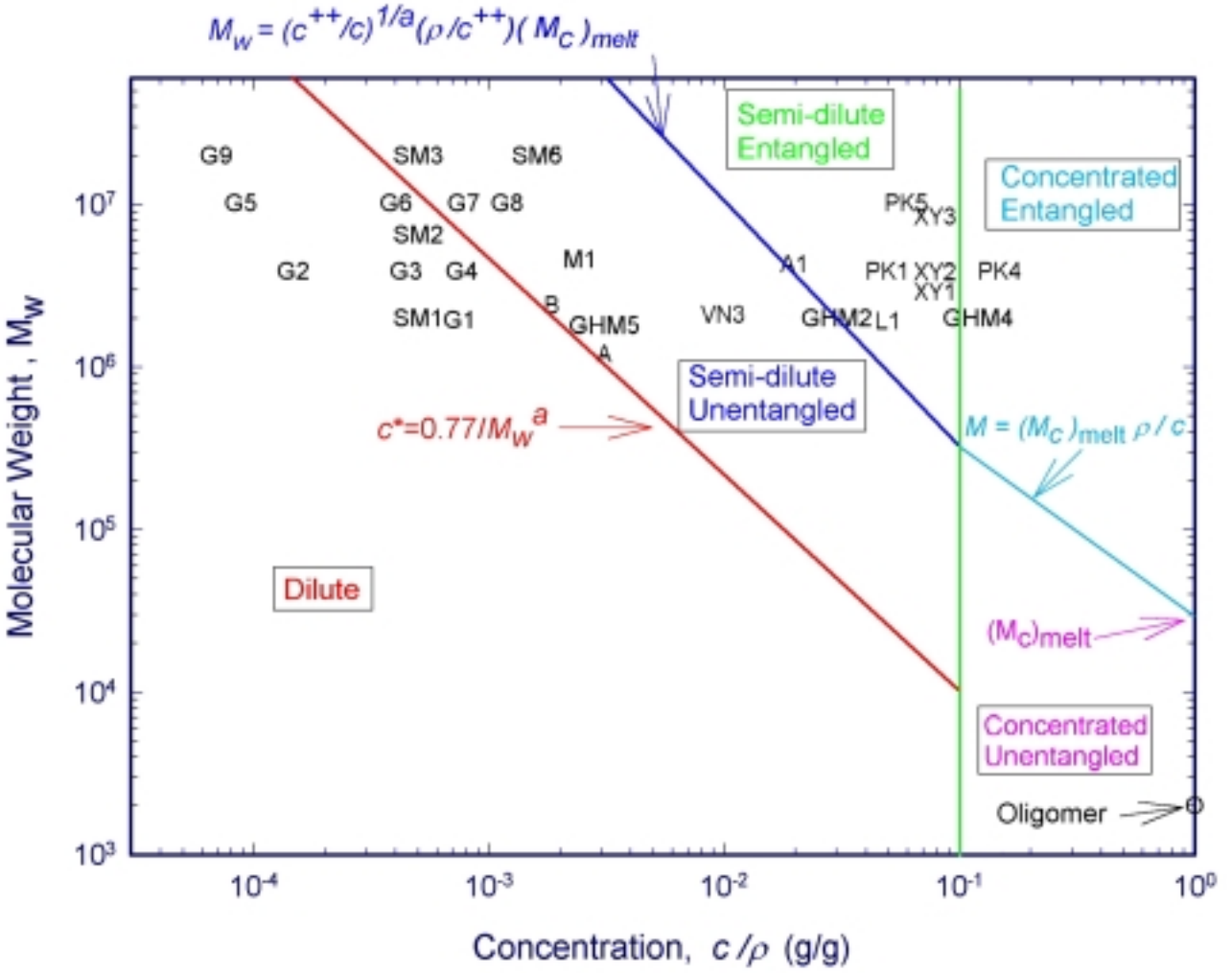

Figure A.1 Graessley diagram showing the concentration (as a dimensionless mass fraction c/ρ) and molecular weight of fluids tested in filament stretching rheometers. The symbols and relevant citations are summarized in Table A.1. Also, some data points and symbols listed in the table has been omitted from the figure for clarity of presentation. The equations for the dividing lines are described in more detail in the text.

The different regions in this plot indicate different equilibrium conditions of the polymer chains in solution. In preparing Figure A.1 we have used parameter values corresponding to polystyrene in a good solvent because the majority of experimental data has been obtained using this macromolecule. The numerical coefficients appearing in the equations of the lines separating these different regions will vary with the specific topology and structure of the primary chain (specifically with the characteristic ratio C_∞, the entanglement molecular weight M_e, and the solvent quality parameter ν); however, the general scaling (and slopes) of the lines are generically valid. Here we briefly summarize these scalings; for more detailed discussions of the different regimes, the reader is referred elsewhere (Doi & Edwards 1986, Larson 1999, Watanabe 1999).

For very low concentrations ($c < c^*$) the polymer chains are isolated from each other in solution and the solution is *dilute*. This overlap concentration (c^*) scales with molecular weight as $c^* \sim M_w^{1-3\nu}$. This can be expressed in the alternate form $c^* \approx 0.77/[\eta]$ where the 'intrinsic viscosity' or 'limiting viscosity number' is given by the Mark-Houwink-Sakurada equation $[\eta] = KM_w^a$ with the exponent $a = 3\nu - 1$. As the concentration of polymer in solution is increased the solution eventually becomes concentrated and hydrodynamic interactions are screened out. DeGennes and Graessley show by scaling arguments that the critical concentration (denoted $c^\ddagger$) for crossover into the concentrated regime is independent of molecular weight (since the long range hydrodynamic interactions of the intermingled chains are all screened out) and is approximately $c^\ddagger/\rho \approx 0.1$. As the molecular weight of the chains increase, they become *entangled* by the constraints of neighboring chains and the molecular motion becomes dominated by curvilinear diffusion or *reptation*. In the melt, the critical molecular weight for entanglement is found to be $2M_e \le M_c \le 5M_e$. In concentrated solutions, the dilution of the number of entanglement interactions leads to a linear variation in the entanglement crossover; $\left(M_c\right)_{\text{soln}} = \left(\rho/c\right)\left(M_c\right)_{\text{melt}}$ for $c^\ddagger \le c \le \rho$. At intermediate values of the concentration the solution is described as *semi-dilute*. In this regime, hydrodynamic interactions may be important below a certain 'screening length' or 'blob' size (ξ) which is dependent on the solvent quality. For very long chains, in the semi-dilute regime entanglement constraints may also be important (Graessley 1980). Experiments for polystyrene suggest that that the crossover between semi-dilute, non-entangled and semi-dilute, entangled systems can be represented by an equation of the form $\left(M_c\right)_{\text{soln}} \approx \left(c^\ddagger/c\right)^{1/(3\nu-1)}\left(\rho/c^\ddagger\right)\left(M_c\right)_{\text{melt}}$ for $c^* < c \le c^\ddagger$ (Osaki, 1985)

From Figure A.1 it can be seen that most filament stretching experiments have employed large macromolecules with $M_w \ge 10^6$ g/mol. in order to explore the effects of chain stretching. Since kinetic theory is most advanced for truly dilute solutions, experiments have also endeavored (not always successfully) to achieve $c[\eta]_0 < 1$. The extensive experiments of Gupta *et al.* (2000) and

Anna *et al*. (2001) thoroughly explored the dilute and semi-dilute unentangled regimes. The concentrated unentangled regime has been investigated by filament stretching experiments using oligomeric solvents which are Newtonian over the range of deformation rates attainable (due to the very short relaxation times of the chains). Less is known about the semi-dilute entangled and concentrated regimes, although recent experiments in high molecular weight polystyrene solutions with concentrations in the 1 – 12 wt.% range have begun to address these regimes (Bhattacharjee *et al*. 2002; Rothstein & McKinley 2002)

Although the Graessley diagram allows one to represent schematically the equilibrium conformation of the polymer chains, it does not capture the viscometric properties of the viscoelastic fluids. These will scale differently with concentration, molecular weight and solvent viscosity in each of the five domains indicated on Figure A.1. An alternative way of representing this information is shown in Figure A.2.

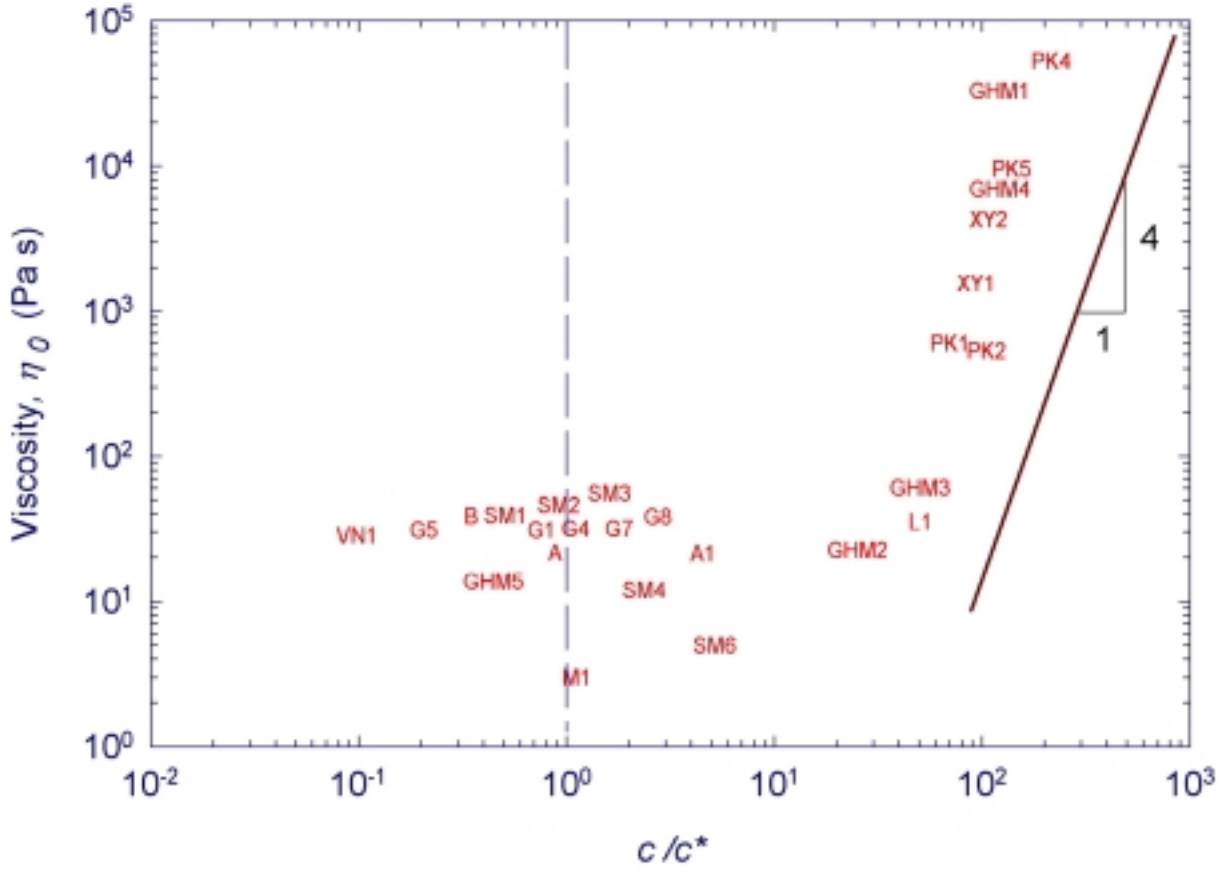

Figure A.2. Concentration of fluids tested (scaled with the overlap concentration c^*) as a function of the zero-shear-rate viscosity of each fluid. Description of the symbols and details of each fluid composition are given in Table A.1.

The zero-shear rate viscosity of the solution measured in steady simple shearing flow is plotted against the dimensionless ratio, c/c^* (corresponding to the degree of overlap between the polymer molecules) for solutions that have been investigated by filament stretching rheometry. The

former (dimensional) viscometric property is important in filament stretching rheometry because large viscosities help minimize inertial, capillary and gravitational corrections (see section 4 in the main review). As the degree of coil overlap decreases, the solvent viscosity typically has to be increased in order to resist these perturbations. Almost all experiments to date have used test fluids with viscosities greater than 3 Pa.s in order to keep the critical strain rate for sagging small (see discussion in section 4.4 and Equation 13). A significant experimental challenge remains in applying filament stretching techniques to more mobile systems.

At higher concentrations, the viscosity of the test fluids are dominated by the entanglements of the high molecular weight chains and filament stretching rheometry is now being used to test ideas from reptation theory. Far above the overlap concentration, reptation gives the following result

$$\eta_0 \approx \tfrac{\pi^2}{4} G_N^0 \tau_e \left(c/\rho\right)^4 \left(M_w/M_{e,melt}\right)^3, \tag{A.1}$$

where G_N^0 is the plateau modulus of the melt and τ_e is the Rouse time for a single entangled segment (see section 3 of review for more details). The zero-shear-rate viscosity thus depends strongly on the concentration and molecular weight. However, substituting for the known scaling $c^* \sim M_w^{1-3\nu}$ we find that

$$\eta_0 \sim \left(c/c^*\right)^4 M_w^{(7-12\nu)}. \tag{A.2}$$

When expressed in this form, the resulting dependence of viscosity on molecular weight is very weak, especially for good solvents ($\nu \approx 0.6$). This leads to an almost universal curve with viscosity varying as $\eta_0 \sim c^4$. This scaling for entangled fluids can be clearly seen in Figure A.2.

LITERATURE CITED

Bhattacharjee PK, Oberhauser JP, McKinley GH, Leal LG, Sridhar T. 2002. Extensional Rheometry of Entangled Solutions. *Macromolecules*: submitted

Doi M, Edwards SF. 1986. *The Theory of Polymer Dynamics*. Oxford: OUP

Graessley WW. 1980. Polymer Chain Dimensions and the Dependence of Viscoelastic Properties on Concentration, Molecular Weight and Solvent Power. *Polymer*. 21: 258-62

Gupta RK, Nguyen DA, Sridhar T. 2000. Extensional Viscosity of Dilute Polystyrene Solutions – Effect of Concentration and Molecular Weight. *Phys. Fluids*. 12(6): 1296-318

Larson RG. 1999. *The Structure and Rheology of Complex Fluids*. New York: Oxford University Press.

Osaki K, Nishimura Y, Kurata M. 1985. Viscoelastic Properties of Semi-dilute Polystyrene Solutions. *Macromolecules*. 18: 1153-7

Rothstein JP, McKinley GH. 2001. A Comparison of the Stress and Birefringence Growth in Dilute and Concentrated Polymer Solutions in Uniaxial Extensional Flow. *J. Non-Newt. Fluid Mech.*(XIIth Int. Workshop Special Issue): submitted

Watanabe H. 1999. Viscoelasticity and Dynamics of Entangled Polymers. *Prog. Polym. Sci.* 24: 1253-40.

No.	Polymer	Concentration (Wt Fraction)	M_w	Solvent	$\dot{\varepsilon}$ $[s^{-1}]$	η_0 [Pa.s]	c/c^*	Symbol	Reference
1	PS	500.0e-6	2.00e+6	Oligomer	2.5-20	39.20	0.52	SM1	Anna, S. L. et al., *J. Rheol.* 45(1):83-114 (2001).
2	PS	500.0e-6	6.50e+6	Oligomer	0.5-1.0	46.10	0.94	SM2	Anna, S. L. et al., *J. Rheol.* 45(1):83-114 (2001).
3	PS	500.0e-6	2.00e+7	Oligomer	0.5-1.0	55.50	1.65	SM3	Anna, S. L. et al., *J. Rheol.* 45(1):83-114 (2001).
4	PS	747.0e-6	1.95e+6	DOP/Oligomer	1~14.6	31.18	0.77	G1	Gupta, R. K.; Nguyen, D. A. and Sridhar, T. *Phys. Fluids* 12(6):1296-1318 (2000).
5	PS	147.0e-6	3.90e+6	DOP/Oligomer	N/A	33.20	0.21	G2	Gupta, R. K.; Nguyen, D. A. and Sridhar, T. *Phys. Fluids* 12(6):1296-1318 (2000).
6	PS	444.0e-6	3.90e+6	DOP/Oligomer	2~14.7	31.68	0.65	G3	Gupta, R. K.; Nguyen, D. A. and Sridhar, T. *Phys. Fluids* 12(6):1296-1318 (2000).
7	PS	767.0e-6	3.90e+6	DOP/Oligomer	1~29.6	31.78	1.12	G4	Gupta, R. K.; Nguyen, D. A. and Sridhar, T. *Phys. Fluids* 12(6):1296-1318 (2000).
8	PS	88.00e-6	1.02e+7	DOP/Oligomer	2~30.2	31.10	0.21	G5	Gupta, R. K.; Nguyen, D. A. and Sridhar, T. *Phys. Fluids* 12(6):1296-1318 (2000).
9	PS	402.0e-6	1.02e+7	DOP/Oligomer	1~7	31.40	0.95	G6	Gupta, R. K.; Nguyen, D. A. and Sridhar, T. *Phys. Fluids* 12(6):1296-1318 (2000).
10	PS	777.0e-6	1.02e+7	DOP/Oligomer	2~9.8	31.80	1.83	G7	Gupta, R. K.; Nguyen, D. A. and Sridhar, T. *Phys. Fluids* 12(6):1296-1318 (2000).
11	PS	1.191e-3	1.02e+7	DOP/Oligomer	0.52	38.49	2.81	G8	Gupta, R. K.; Nguyen, D. A. and Sridhar, T. *Phys. Fluids* 12(6):1296-1318 (2000).
12	PS	69.00e-6	2.00e+7	DOP/Oligomer	0.8~30.4	31.89	0.23	G9	Gupta, R. K.; Nguyen, D. A. and Sridhar, T. *Phys. Fluids* 12(6):1296-1318 (2000).
13	PS	2.300e-3	2.00e+6	DOP/Oligomer	0.3~3	12.00	2.40	SM4	Solomon, M. J. and Muller, S. J., *J. Rheol.* 40(5):837-856 (1996).
14	PS	1.600e-3	2.00e+7	DOP/Oligomer	0.3~3	4.00	5.28	SM5	Solomon, M. J. and Muller, S. J., *J. Rheol.* 40(5):837-856 (1996).
15	PS	1.600e-3	2.00e+7	TCP/Oligomer	0.3~3	5.00	5.28	SM6	Solomon, M. J. and Muller, S. J., *J. Rheol.* 40(5):837-856 (1996).
16	PS	0.05	3.90e+6	DOP	0.1~1	600.00	71.4	PK1	Bhattacharjee, P. K et al. *Macromolecules* in press (2001).
17	PS	0.07	3.90e+6	DBP	0.5~5.8	533.00	107.1	PK2	Bhattacharjee, P. K et al. *Macromolecules* in press (2001).
18	PS	0.10	3.90e+6	DEP	0.1~14	4570.00	145.8	PK3	Bhattacharjee, P. K et al. *Macromolecules* in press (2001).
19	PS	0.15	3.90e+6	DEP	0.05~4	53000.00	218.7	PK4	Bhattacharjee, P. K et al. *Macromolecules* in press (2001).
20	PS	0.06	1.02e+7	DBP	0.03~1.75	9560.00	141.4	PK5	Bhattacharjee, P. K et al. *Macromolecules* in press (2001)
21	PS	0.08	2.89e+6	TCP	0.1~6	1550.00	95.4	XY1	Ye, X.; Larson, R. G.; Pattamaprom, C. and Sridhar, T. in preparation (2002)

22	PS	0.08	3.84e+6	TCP	0.6~3	4300.00	109.9	XY2	Ye, X.; Larson, R. G.; Pattamaprom, C. and Sridhar, T. in preparation (2002)
23	PS	0.08	8.42e+6	TCP	0.1~0.8	49000.00	162.8	XY3	Ye, X.; Larson, R. G.; Pattamaprom, C. and Sridhar, T. in preparation (2002)
24	PS	0.12	2.00e+6	TCP	0.5-5.0	33000.00	125.3	GHM1	Mckinley, G.H., Brauner O., Yao M.-Y., *Korea-Australia Rheol. J*, 13: 29-35, 2001
25	PS	0.03	2.00e+6	Oligomer	1~2	22.75	26.1	GHM2	Rothstein, J.P. and McKinley G.H., *J. Non-Newt. Fluid Mech.*, in press 2002.
26	PS	0.05	2.00e+6	TCP	3.00	60.90	52.2	GHM3	Rothstein, J.P. and McKinley G.H., *J. Non-Newt. Fluid Mech.*, in press 2002.
27	PS	0.12	2.00e+6	TCP	1.00	6930.00	125.3	GHM4	Rothstein, J.P. and McKinley G.H., *J. Non-Newt. Fluid Mech.*, in press 2002
28	PS	1.00	2000.00		1-3			O	Spiegelberg et al *J. Non-Newt. Fluid Mech.,* 64: 229-267 (1996)
29	PS	0.05	1.92e+6	TCP/Oligomer	4.68	35.25	51.1	L1	Li et al *J. Non-Newt. Fluid Mech.*, 74: 151-193 (1998)
30	PIB	3.100e-3	1.80e+6	C14/PB	1~4.2	13.76	0.46	GHM5	Spiegelberg et al *J. Non-Newt. Fluid Mech.,* 64: 229-267 (1996)
31	PIB	600.0e-6	2.11e+6	Kerosene/PB	1~6	28.50	0.1	VN1	van Nieuwkoop, J. et al*, J. Non-Newt. Fluid Mech.,* 67: 105-124 (1996).
32	PIB	1.850e-3	2.11e+6	Kerosene/PB	1~6	34.20	0.3	VN2	van Nieuwkoop, J. et al*, J. Non-Newt. Fluid Mech.,* 67: 105-124 (1996).
33	PIB	0.01	2.11e+6	Kerosene/PB	1~6	48.30	1.6	VN3	van Nieuwkoop, J. et al*, J. Non-Newt. Fluid Mech.,* 67: 105-124 (1996).
34	PIB	1.850e-3	4.30e+6	Toluene/PB	1~6	24.20	0.4	VN4	van Nieuwkoop, J. et al*, J. Non-Newt. Fluid Mech.,* 67: 105-124 (1996).
35	PIB	3.100e-3	1.20e+6	C14/PB		21.60	0.89	A	Orr N.V. and Sridhar, T. *, J. Non-Newt. Fluid Mech.*, 67: 77-104 (1996).
36	PIB	1.850e-3	2.40e+6	Kerosene/PB	1~4	38.80	0.35	B	Orr N.V. and Sridhar, T. *, J. Non-Newt. Fluid Mech.*, 67: 77-104 (1996).
37	PIB	2.440e-3	4.60e+6	Kerosene/PB		3.00	1.14	M1	Tirtaatmadja, V. and Sridhar, T., *J. Rheol.* 37(6):1081-1102 (1993)
38	PIB	0.02	4.30e+6	Decalin		21.50	4.6	A1	Tirtaatmadja, V. and Sridhar, T., *J. Rheol.* 37(6):1081-1102 (1993)
39	PIB	0.03	1.20e+6	Decalin/PB	1.7~7.5	13.60	3.7	S1	Ooi Y.W. and Sridhar, T*., J. Non-Newt. Fluid Mech*., 52:153-162 (1993) .

Table A.1 Details of the composition of viscoelastic fluids containing linear homopolymers that have been tested to date in the filament stretching rheometer. The polymers used include polyisobutylene (PIB) and Polystyrene (PS). Solvents include Dioctyl Phthalate (DOP); Dibutyl Phthalate (DBP); Diethyl Phthalate (DEP); Tricresyl Phosphate (TCP); low mol. weight (oligomeric) styrene, kerosene (K), tetradecane (C14) and polybutene (PB). Abbreviated literature citations are given in the final column; full details can be found in the bibliography at the end of the main review.

APPENDIX B: Constitutive Models for Polymer Solutions

In this appendix we provide an expanded discussion of the predictions of simple constitutive theories relevant to the extensional flow of polymer solutions generated by filament stretching rheometers.

The viscoelastic nature of polymeric materials means that the extra stress in a fluid element depends on the entire history of deformation experienced by that element. The stress can therefore be expressed as a functional of the velocity gradient, time and other microstructural details. In the present review we are principally concerned with dilute polymer solutions, and one has to deal primarily with the topology of a single chain plus intramolecular and polymer-solvent interactions. This is in contrast to the inter-molecular effects that dominate the rheology of concentrated systems. Bird (1982) has reviewed the use of molecular models derived from kinetic theory in extensional flows and more recent developments are also provided by Bird & Wiest (1995). For more complete discussions of constitutive modeling in other flows see for example the texts by Bird et al 1987a,b; Larson, 1988; Tanner, 2000).

A hierarchical description of the fluid microstructure that can be progressively and systematically reduced in dimensionality ('coarse-grained') is shown in Figure 1 of the text. By correctly incorporating the molecular details, specific predictions (e.g. the scalings of the relaxation time and viscosity with molecular weight and concentration) can be obtained. The parameter values in this figure are for a typical polystyrene (PS) molecule with a molecular weight of 2.25×10^6 g/mol and show the dramatic reduction in the number of internal variables that can be achieved by appropriate coarse graining.

The enormous range of length scales (and time scales) evident in the figure, permit a variety of modeling approaches. In an actual polymer molecule, the bond lengths and angles are restricted to quite narrow ranges (Flory, 1969) and the internal structure is highly repetitive. A polymer chain can thus be represented as a set of n beads joined at freely rotating connectors (of fixed bond angle) by mass-less rods of length l. Each bead represents the center of mass corresponding to a monomer unit and the length of each rod connecting successive beads corresponds to the carbon-carbon bond length between monomers. Rotations about each bond are sterically hindered by the chain topology and the presence of side groups and these effects are encapsulated in the characteristic ratio C_∞. On larger scales, however, successive bond orientations become progressively uncorrelated. Further coarse graining thus yields the *freely jointed bead-rod model* of Kuhn in which N rods (each comprising several monomers) of length b are connected. This freely jointed bead-rod chain can be further simplified by replacing a portion of the chain consisting of several rods by a Hookean (or non-Hookean) spring describing the entropic forces acting on that segment of the chain. This *bead-spring model* of M beads and springs allows the configurational dynamics of a polymer chain to be investigated without the computational difficulties associated with the fixed bond-lengths of the bead-rod model. The bead-spring chains are able to capture some of the essential features of real polymer molecules, such as orientability, extensibility and a spectrum of internal relaxational degrees of freedom. The Rouse and Zimm models represent two limiting situations depending on the magnitude of the hydrodynamic interaction between the beads.

Although analytically tractable in some simple flows, these models are still too complex for large numerical simulations of non-Newtonian flows. They can however be simplified still further by replacing all of the individual monomers by a single *dumbbell*; i.e. a mass-less linear (or nonlinear) spring with the mass of the chain evenly distributed between two point masses at either end of the spring. These 'beads' are also the locus of all hydrodynamic interactions between the chain and the solvent. When external motion is imposed, the chain segments are subjected to hydrodynamic drag forces, an entropic spring force, Brownian motion and appropriate constraints. Starting with a chosen microstructural model, a stochastic Langevin equation can be written for the balance of forces on each bead in the chain or dumbbell (see the text by Öttinger, 1996 for further details). Equivalently this can be represented as a diffusion or Smoluchowski equation for the probability distribution function of the internal coordinates, $\psi(Q,t)$, where Q is the end-to-end vector. The solution of these equations typically proceeds via simplifying 'closure approximations' for the ensemble averages, or numerical solution of the diffusion equation or Brownian dynamics simulations of the Langevin equation (Herrchen & Öttinger, 1997; Keunings, 1997). The consequences of these approximations and numerical schemes are only now being understood and this continues to be an active area of research (Van den Brule, 1993; Lielens et al 1998; Ghosh et al. 2001).

B.2 Constitutive Response in Homogeneous Elongation Flow

We wish to consider the response of a prototypical viscoelastic constitutive equation in a homogeneous extensional flow. In an irrotational flow with kinematics given by eq. (1) in the main text, the differential equations for the evolution in the microstructural deformation and the polymeric stress become particularly simple to solve since the deformation gradient and stress tensors become diagonal.

The transient extensional response of the 'rubber-like liquid' (corresponding to a Hookean bead-spring chain with a discrete spectrum of N_m relaxation times) was first considered by Chang & Lodge, (1971) and was shown to quite accurately capture experimental measurements of the transient extensional response in polymeric melts. For all viscoelastic fluids in the limit of very low extension rates, simple fluid theory (Bird et al 1987a) shows that the steady state extensional viscosity must approach three times the zero-shear viscosity. For a linear viscoelastic material with a discrete spectrum of relaxation times and moduli $\{G_i, \lambda_i\}$ the transient Trouton ratio (i.e. the dimensionless extensional stress growth coefficient) can be shown to be

$$Tr^+ \equiv \frac{\eta_E^+(\dot{\varepsilon}_0, t)}{\eta_0} = \frac{3\eta_s + \sum_{i=1}^{N_m} 3\eta_i \left(1 - \exp\left[-t/\lambda_i\right]\right)}{\eta_0} \tag{B.1}$$

where the contribution to the total viscosity of the ith mode is given by $\eta_i = G_i \lambda_i$ and η_s is the contribution from the Newtonian solvent (if present). The total steady-state viscosity of the fluid in the limit of zero deformation rate is given by

$$\eta_0 = 3\eta_s + \sum_{i=1}^{N_m} 3\eta_i \tag{B.2}$$

Verifying that this linear viscoelastic response (eq. B.1) is actually obtained at low deformation rates $\lambda_i \dot{\varepsilon}_0 << 1$ is a very stringent test of transient filament stretching experiments for both melts and concentrated solutions (Münstedt & Laun, 1979; Meissner, 1985; McKinley et al. 2001).

At short times $t << \lambda_i$, the transient Trouton ratio (or dimensionless extensional stress growth coefficient) in any polymeric material is thus

$$\lim_{t=0^+} Tr^+ = \frac{3\eta_s}{\eta_0}$$

For dilute solutions (of concentration $c < c^*$) the polymeric contribution to the zero-shear rate viscosity is small and of order *O(c)* (or formally $\eta_p \equiv (\eta_0 - \eta_s) = [\eta]c$ where $[\eta]$ is the intrinsic viscosity), and thus the Trouton ratio at the beginning of a filament stretching experiment should be very close to three as can be observed in a number of the figures in the review (cf. Figs 7,11). However as the material becomes entangled and the contribution of the solvent to the total stress in the fluid decreases, the initial value of the Transient Trouton ratio in fact decreases to values much less than three.

In the limit of 1 relaxation mode the linear bead-spring chain model reduces to the Hookean dumbbell model (i.e. a dumbbell with a linear connector force) or, equivalently, the Oldroyd-B equation of continuum mechanics (Bird et al. 1987a,b). For clarity, we focus on this topmost or most 'coarse-grained' level in Figure 1 and consider the effects of finite extensibility in the spring and anisotropy in the drag acting on the chain. After appropriate closure approximations (Bird et al. 1987b, Herrchen & Öttinger, 1997) the conformation of the molecules can be presented by a single evolution equation of the form

$$\frac{D\boldsymbol{A}}{Dt} - \left\{ \nabla \boldsymbol{v}^T \cdot \boldsymbol{A} + \boldsymbol{A} \cdot \nabla \boldsymbol{v} \right\} = -\frac{1}{\lambda}\left[\boldsymbol{I} + \alpha(\boldsymbol{A} - \boldsymbol{I}) \right] \cdot \left[f(tr\boldsymbol{A})\boldsymbol{A} - \boldsymbol{I} \right], \tag{B.3}$$

where the conformation tensor $\boldsymbol{A} \equiv \langle \boldsymbol{QQ} \rangle / (Q_{eq}{}^2 / 3)$ is the ensemble average of the dyadic product of the dumbbell connector vector scaled with the equilibrium size of the freely jointed chain, $Q_{eq}^2 = Nb^2$. The left hand-side of eq. B.3 is the familiar upper-convected derivative of the conformation tensor. The single relaxation time of the chain is denoted by λ, α is a measure of the anisotropy in the drag acting on the dumbbell as it orients and elongates and $f(tr\boldsymbol{A})$ is the nonlinearity of the spring.

The total deviatoric stress arising from the solvent and the presence of the deformed dumbbells can be found from the conformation tensor to be

$$\boldsymbol{\tau} = \boldsymbol{\tau}_s + \boldsymbol{\tau}_p = \eta_s \dot{\boldsymbol{\gamma}} + \nu k_B T \left[f(tr\boldsymbol{A})\boldsymbol{A} - \boldsymbol{I} \right], \tag{B.4}$$

where ν is the number density of polymer chains, k_B is Boltzmann's constant and T is the absolute temperature. When $\alpha = 0$ and $f(tr\boldsymbol{A}) = \left[1 - tr\boldsymbol{A} / 3N\right]^{-1}$, eqs. (B.3)–(B.4) reduce to the FENE-P model

and when $\alpha \neq 0$, $f(tr\boldsymbol{A}) = 1$ the equations are identical to the Giesekus model. In the limit $\alpha = 0$ and $f(tr\boldsymbol{A}) = 1$ the model becomes the Hookean (i.e. linear elastic) dumbbell model.

In an irrotational flow with kinematics given by eq. (1) in the text, the differential equations for the evolution in the microstructural deformation become particularly simple to solve. Combining eqs. (1), (B.3) and (B.4) leads to the following expression for the transient extensional viscosity of the Hookean dumbbell model

$$\eta_E^+(\dot{\varepsilon}_0, t) = 3\eta_s + \frac{2\nu k_B T\lambda}{(1-2\lambda\dot{\varepsilon}_0)}\left[1-\exp\left(-\left(1-2\lambda\dot{\varepsilon}_0\right)t/\lambda\right)\right] + \frac{\nu k_B T\lambda}{\left(1+\lambda\dot{\varepsilon}_0\right)}\left[1-\exp\left(-\left(1+\lambda\dot{\varepsilon}_0\right)t/\lambda\right)\right], \qquad \text{(B.5)}$$

The dimensionless product in eq. (B.5) is the *Deborah number*, $De = \lambda\dot{\varepsilon}_0$, which can be positive or negative for uniaxial or biaxial flows respectively. For $|De| << 1$ eq. (B.5) reduces to the linear viscoelastic prediction of eq. (B.1) with $N_{modes} = 1$ and $\eta_0 = \eta_s + \nu k_B T\lambda$. For values $-1 < De < 0.5$, eq. (B.5) predicts the extensional viscosity approaches a steady state value that is *O(De)* above the linear viscoelastic limit; however, for $De \geq 0.5$, the uniaxial extensional viscosity grows without bound. This corresponds to a 'coil-stretch transition' at a critical value of the Deborah number as first described by de Gennes (de Gennes, 1979). This transition has since been confirmed in numerous experiments, perhaps most unambiguously in the single molecule imaging results of Chu & co-workers (Perkins et al 1997; Smith and Chu 1998). On a microscopic scale the strength of the external flow overwhelms the restoring effects of Brownian motion and the linear connector force and the molecule unravels without limit.

At large strains, the dumbbell conformation (and associated polymeric stress) are dominated by the *zz*-component which can be expressed in the simple form

$$\lim_{\substack{De>0.5 \\ \varepsilon>1}} \left\{\frac{\tau_{zz}}{\nu k_B T}\right\} \equiv A_{zz} = \frac{1}{\left(1-0.5/De\right)}\left[\exp\left(2\varepsilon(1-0.5/De)\right)-1\right], \qquad \text{(B.6)}$$

where we have substituted the identity $\varepsilon \equiv \dot{\varepsilon}_0 t$ to emphasize that the stress growth is dominated by the exponential growth in the macroscopic stretch of the material fluid elements. On a semi-logarithmic plot of log(stress) against strain the tensile stress (or the transient Trouton ratio) thus increases exponentially with a slope given by $2(1-0.5/De)$. This relative insensitivity to the rate of stretching is shown quite clearly in Figure B.1.

The unraveling of the molecules of course cannot continue *ad infinitum* and eventually the chain is fully unraveled. Such effects can be captured by incorporating finite extensibility into the spring connector force. The resulting equations (B.3)–(B.4) are nonlinear and must be solved numerically. However in a strong stretching flow with $De > 0.5$, the response is initially given by eq. (B.5). At very large strains, the stress saturates at a steady state value given by

$$\tau_{zz} = 2\nu k_B T L^2\,\lambda\dot{\varepsilon}_0\left[(1-3/L^2) - 0.5/De + O(De^{-2})\right], \qquad \text{(B.7)}$$

where $L = Q_{\max}/Q_{eq} = \sqrt{3N}$ is the extensibility of the linear chain. The extensional viscosity of the elongated chains is thus a factor of L^2 larger than the polymeric contribution to the shear viscosity ($\eta_p = \nu k_B T \lambda$). Numerical simulations (Doyle et al. 1998; Ghosh et al. 2001) show that this expression agrees well with full numerical simulations for bead-rod and bead-spring chains.

As we discuss in the text, an issue in the design of filament stretching devices is the initial inhomogeneity in the kinematics induced by the no-slip condition at the endplates of the device. In a Newtonian fluid, scaling arguments and numerical simulations show that the importance of such variations decay as the filament becomes increasingly slender, however this is not the case for polymeric materials undergoing sufficiently rapidly stretching. Direct integration of the Hookean dumbbell equation for a series of non-interacting annular rings of polymeric material with specified initial stretches $A_{zz}^{(0)}(r)$ undergoing ideal uniaxial elongation gives

$$\frac{\tau_{zz}(r,t)}{\nu k_B T} = A_{zz}(r,t) = \left[A_{zz}^{(0)}(r) + \frac{1}{\left(1 - 0.5/De\right)} \right] \exp\left(2\varepsilon\left(1 - 0.5/De\right)\right) - \frac{1}{\left(1 - 0.5/De\right)}. \qquad \text{(B.8)}$$

Examining eq. (B.8) it is clear that for $De > 0.5$ the initial stretched configuration never decays. Since the magnitude of the stretch is directly connected to the polymeric stress τ_{zz}, the evolution in this radial gradient leads to the development of sharp boundary layers in the axial stress near the free surface of the filament (profiles of these stress boundary layers are shown in Yao et al. 1998b and are discussed further by Arun Kumar & Graham 2000). Experimental measurements near the midplane of integrated quantities such as the birefringence or the total axial force will thus be appropriately weighted averages of this radial distribution in the stress (Sizaire et al. 1999). It is thus important to optimize the initial aspect ratio of the liquid bridge samples used in experiments.

Simulations by Harlen (unpublished results, 1996) have shown that the complex radial variations induced at short times by the inward free-surface motion are indeed simply convected forward in time in self-similar form as suggested by eq. (B.8). Harlen also found that the effects of such radial variations can be minimized by selecting $\Lambda_0 \approx 1$. This is indeed the value now most commonly used in filament stretching experiments. Non-zero initial conditions also affect the rate of elasto-capillary self-thinning indicated in filament breakup studies (Kolte & Szabo, 1999) and thus dramatically affect the time to breakup observed in a microfilament rheometer (Anna & McKinley, 2001).

This sensitivity to initial molecular configurations suggests a new way of systematically probing the role of pre-shearing and other upstream deformation histories on commercially important Lagrangian-unsteady extensional flows such as fiber-spinning (Ferguson et al 1998). Controlled levels of molecular pre-conditioning can be achieved by imposing a controlled rotational shear flow or oscillatory squeeze-flow (Anna & McKinley, 2000).

References

Anna SL, McKinley GH. 2000. In *Proceedings of the. XIIIth Int. Cong. Rheology*, Vol. 1, ed. DM Binding, NE Hudson, J Mewis, J-M Piau, CJS Petrie, P Townsend, MH Wagner, K Walters, pp. 360-2. Cambridge (UK): British Society of Rheology

Arun Kumar K, Graham MD. 2000. Buckling Instabilities in Models of Viscoelastic Free-Surface Flows. *J. Non-Newt. Fluid Mech.* 89: 337-51

Bird RB. 1982. Polymer Kinetic Theories and Elongational Flows. *Chem. Eng. Commun.* 16: 175-87

Bird RB, Armstrong RC, Hassager O. 1987a. *Dynamics of Polymeric Liquids. Volume 1: Fluid Mechanics*. New York: Wiley Interscience;

Bird RB, Curtiss CF, Armstrong RC, Hassager O. 1987b. *Dynamics of Polymeric Liquids. Volume 2: Kinetic Theory*. New York: Wiley Interscience.

Bird RB, Wiest JM. 1995. Constitutive Equations for Polymeric Liquids. *Ann. Rev. Fluid Mech.* 27: 169-93

Chang H, Lodge AS. 1972. Comparison of Rubberlike-Liquid Theory with Stress-Growth Data for Elongation of a low-Density Branched Polyethylene Melt. *Rheol. Acta*. 11: 127-

de Gennes P-G. 1979. *Scaling Concepts in Polymer Physics*. Ithaca: Cornell University Press.

Doyle P, Shaqfeh ESG, McKinley GH, Spiegelberg SH. 1998. Relaxation of Dilute Polymer Solutions Following Extensional Flow. *J. Non-Newt. Fluid Mech.* 76(1-3): 79-110

Ferguson J, Hudson NE, Forsyth JF. 1998. Transient Extensional Rheology and the Influence of Strain History. *J. Non-Newtonian Fluid Mech.* 79: 213-23

Flory PJ. 1969. *Statistical Properties of Chain Molecules*. New York: Wiley Interscience.

Ghosh I, McKinley GH, Brown RA, Armstrong RC. 2001. Deficiencies of FENE Dumbbell Models in Describing the Rapid Stretching of Dilute Polymer Solutions. *J. Rheol.* 45(3): 721-58

Herrchen M, Öttinger HC. 1997. A Detailed Comparison of Various FENE Dumbbell Models. *J. Non-Newtonian Fluid Mech.* 68(1): 17-42

Keunings R. 1997. On the Peterlin Approximation for Finitely Extensible Dumbbells. *J. Non-Newt. Fluid Mech.* 68: 85-100

Kolte MI, Szabo P. 1999. Capillary Thinning of Polymeric Filaments. *J. Rheology*. 43(3): 609-26

Larson RG. 1988. *Constitutive Equations for Polymer Melts and Solutions*. Boston: Butterworths.

Lielens G, Halin P, Jaumain I, Keunings R, Legat V. 1998. New Closure Approximations for the Kinetic Theory of Finitely Extensible Dumbbells. *J. Non-Newt. Fluid Mech.* 76: 249-80

McKinley GH, Brauner O, Yao M. 2001. Kinematics of Filament Stretching in Dilute and Concentrated Polymer Solutions. *Korea-Aust. Rheol. J.* 13(1): 29-35

Meissner J. 1985. Experimental Aspects in Polymer Melt Elongational Rheology. *Chem. Eng. Commun.* 33: 159-80

Münstedt H, Laun HM. 1979. Elongational Behavior of a Low Density Polyethylene Melt II. Transient Behaviour in constant stretching and tensile creep experiments. Comparison with shear data. Temperature dependence of the elongational properties. *Rheol. Acta*. 18: 492-504

Öttinger HC. 1996. *Stochastic Processes in Polymeric Liquids*. Berlin: Springer-Verlag.

Perkins TT, Smith DE, Chu S. 1997. Single Polymer Dynamics in an Elongational Flow. *Science*. 276: 2016-21

Sizaire R, Lielens G, Jaumain I, Keunings R, Legat V. 1999. On the Hysteretic Behavior of Dilute Polymer Solutions in Relaxation Following Extensional Flow. *J. Non-Newt. Fluid Mech.* 82(2-3): 233-54

Smith DE, Chu S. 1998. The Response of Flexible Polymer Coils to a Sudden High Strain Rate Flow. *Science*. 281: 1335-40

Tanner RI. 2000. *Engineering Rheology*. Oxford: Clarendon. (2nd Edition).

van den Brule BHAA. 1993. Brownian Dynamics Simulation of Finiteley Extensible Bead-Spring Chains. *J. Non-Newtonian Fluid Mech.*: 357-78

Yao M, McKinley GH. 1998. Numerical Simulation of Extensional Deformations of Viscoelastic Liquid Bridges in Filament Stretching Devices. *J. Non-Newtonian Fluid Mech.* 74((1-3)): 47-88

Wiest JM. 1989. A Differential Constitutive Equation for Polymer Melts. *Rheol. Acta*. 28: 4-12